J Fluoresc (2011) 21:1689–1695
DOI 10.1007/s10895-011-0861-z

ORIGINAL PAPER

Fluorescence Study of Lipid Bilayer Interactions of Eu(III) Coordination Complexes

Olga K. Kutsenko · Valeriya M. Trusova · Galyna P. Gorbenko · Todor Deligeorgiev · Aleksey Vasilev · Stefka Kaloianova · Nedyalko Lesev

Received: 20 December 2010 / Accepted: 13 February 2011 / Published online: 22 February 2011

Abstract The interaction between Eu(III) tris-β-diketonato coordination complexes (EC), displaying antitumor activity, and lipid vesicles composed of zwitterionic lipid phosphatidylcholine has been studied using fluorescence spectroscopy techniques. To characterize EC-membrane binding, several fluorescent probes, including pyrene, Prodan and 1,6-diphenyl-1,3,5-hexatriene, have been employed. It has been found that EC display effective partitioning into lipid phase, giving rise to structural modifications of both polar and nonpolar lipid bilayer regions, viz. enhancement of membrane hydration and increase in tightness of lipid chain packing. The fact that EC accumulating in lipid bilayer are incapable of inducing significant disruption of membrane structural integrity creates strong prerequisites for development of liposomal nanocarriers of these potential antitumor drugs. Such a possibility is also corroborated by the observation that EC membrane incorporation does not prevent lipid bilayer partitioning of long-wavelength squaraine dyes which represent promising candidates for visualization of liposome biodistribution.

O. K. Kutsenko · V. M. Trusova · G. P. Gorbenko
Department of Biological and Medical Physics,
V.N. Karazin Kharkov National University,
4 Svobody Sq.,
Kharkov 61077, Ukraine

T. Deligeorgiev · A. Vasilev · S. Kaloianova · N. Lesev
Department of Applied Organic Chemistry, Faculty of Chemistry,
University of Sofia,
1164 Sofia, Bulgaria

V. M. Trusova (✉)
19–32 Geroyev Truda St.,
Kharkov 61144, Ukraine
e-mail: valtrusova@yahoo.com

Keywords Eu(III) coordination complexes · Fluorescence spectroscopy · Lipid bilayer · Europium complexes · Liposomal nanocarriers · NIR dyes

Introduction

Within the past decades biomedical research has been revolutionized by extensive development of a diversity of multifunctional nanostructures, particularly, liposome-based drug delivery systems [1–3]. These systems have found numerical application in different therapeutic areas, including treatment of tuberculosis [4], malignant growth [5–8], immune system diseases [9], antibiotic delivery [10], etc. Owing to similarity between liposome and cell membrane composition, lipid vesicles are almost completely assimilated by an organism or quickly removed from it [11]. The agents encapsulated into liposomes display reduced harmful effects compared to their free forms. Lipid vesicles facilitate drug uptake by an organism [5, 9], prevent its chemical degradation and transformation [6]. Furthermore, liposomal formulations prolong shelf life of drugs [8, 10]. A number of approaches, such as polymer inclusion, variations in lipid composition [10], pH, temperature [2, 10–13] are currently used to increase stability of liposome-based drug nanocarriers.

Lanthanide coordination complexes have found numerous applications in different areas of biological and clinical sciences. Due to their remarkable luminescence properties (large Stokes shift, long fluorescence lifetime) these compounds are widely used in immunoassay [14–16], DNA hybridization assay [16], molecular diagnostics [14], liposome visualization in biological media [17]. Various lanthanide chelates are utilized in EPR and NMR analyses as lipid bilayer alignment agents [18]. In addition, they display antibacterial, antifungicidal and antitumor activity

[19–21]. Eu(III) tris-β-diketonates (EC) (Fig. 1) with common formula $Eu(L)_3Int$, where L is acetyl acetone, thenoyltrifluoroacetone, benzoylacetone, dibenzoylmethane and Int is 1,10-phenantroline or 2,20-bipyridine are novel compounds with high antineoplastic activity due to their ability to intercalate into DNA [22]. Encapsulation of these compounds into the lipid vesicles represents a perspective way of their therapeutic application. However, clinical use of EC liposomal formulation ought to be appended with elucidating the nature of EC-lipid bilayer interactions. Information in this regard seems to be of importance for at least two reasons. First, molecular details of EC-membrane interactions may prove useful for effective and stable encapsulation of EC into lipid vesicles. Second, EC-induced changes in physicochemical properties of lipid bilayer may provoke undesirable side effects.

Meanwhile, to the best of our knowledge, the process of EC-lipid association and its implications are so far poorly investigated. The present study was undertaken to fill this gap. Our goal was twofold: a) to examine EC influence on the structural state of phosphatidylcholine (PC) model membranes using fluorescent probes 6-propionyl-2-dimethylaminonaphthalene (Prodan), pyrene and 1,6-diphenyl-1,3,5-hexatriene (DPH), and b) to evaluate the possibility of liposome co-loading with EC and NIR dyes which can serve as imaging or photosensitizing agents.

Experimental

Materials

Egg yolk phosphatidylcholine was purchased from Biolek (Kharkov, Ukraine). Phospholipid gave single spot by thin layer chromatography in the solvent system chloroform: methanol:acetic acid:water, 25:15:4:2, *v/v*. SQ-1, SQ-2, SQ-3, V2 and Eu(III) coordination complexes were synthesized as described previously [22–24]. Pyrene, 1,6-diphenyl-1,3,5-hexatriene (DPH) and 6-propionyl-2-dimethylamino-naphthalene (Prodan) were from Sigma (Germany). All other chemicals were of analytical grade.

Preparation of Lipid Vesicles

Unilamellar lipid vesicles of two types, composed of neat PC and PC with embedded EC (EC-to-lipid molar ratio was 1:50) were prepared using the extrusion technique [25]. Appropriate amounts of lipid ethanol solution and EC solution in equimolar ethanol:methanol mixture, were evaporated to dryness under vacuum to remove organic solvent. The obtained lipid films were subsequently hydrated with 1.2 ml of 5 mM Na-phosphate buffer (pH 7.4). The resulting dispersions were extruded through a 100 nm pore size polycarbonate filter (Nucleopore, Pleasanton, CA). The lipid concentration determined according to the procedure of Bartlett [26] was 10 mM. Liposomes with incorporated EC will be referred to here as PC_{EC}.

Spectroscopic Measurements

All measurements were performed in 5 mM sodium phosphate buffer, pH 7.4, at room temperature. Fluorescence measurements were performed with CM 2203 (Solar, Belarus) and Perkin Elmer LS55 (UK) spectrofluorimeters. Excitation wavelengths were 340 nm for pyrene, 350 nm for DPH and Prodan, 640 nm for SQ-1, 660 nm for SQ-2, 620 nm for SQ-3, and 685 nm for V2. Excitation and emission slit widths were set at 2.5 nm for pyrene and Prodan fluorescence measurements, 5 nm for SQ-1, V2, SQ-2, 10 nm for SQ-3 fluorescence and DPH anisotropy measurements.

Results and Discussion

DPH Fluorescence Anisotropy Study

To obtain comprehensive information about EC impact on lipid bilayer properties, 11 fluorescent probes, located in

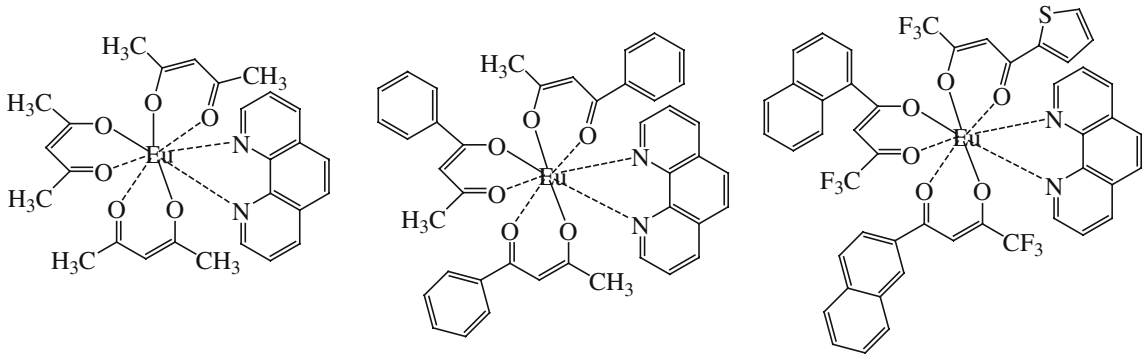

Fig. 1 Structure of Eu(III) coordination complexes

different membrane regions, have been used. Eu(III) complexes were represented by EC1, EC3 and EC6, whose chemical structures are shown in Fig. 1. Since PC is a zwitterionic phospholipid and EC are uncharged hydrophobic molecules, it seemed reasonable to suppose that interactions of Eu(III) chelates with lipid bilayer are driven mainly by hydrophobic forces. Therefore, at the first step of the study we analyzed EC influence on nonpolar membrane region by measuring DPH fluorescence anisotropy. In the aqueous phase DPH virtually does not dissolve, it emits only in membrane-bound state [27]. In lipid bilayer DPH resides in hydrophobic region [28] where there exist two populations of the probe molecules, disposed either along lipid tails or parallel to bilayer surface [29–31]. DPH fluorescence anisotropy reflects the changes in probe rotational diffusion rate, which, in turn, characterizes the compactness of lipid chain packing [26, 32–34]. In close-packed environment DPH fluorescence is characterized by high anisotropy value which decreases with reducing the tightness of acyl tail packing.

As seen from Table 1, EC effect on DPH anisotropy depends on EC structure. EC1 and EC3 embedment into PC bilayer was followed by anisotropy increase by 26% and 19%, respectively, while EC6 decreased this parameter by 14%. Anisotropy increase implies restriction of DPH rotational mobility, i.e. increase of lipid chain packing density in PC bilayer upon insertion of EC1 and EC3. Average sizes of these compounds were estimated to be 1.2 nm (EC1) and 1.5 nm (EC3). While analyzing the experimental data, one should bear in mind that lipid–lipid interactions can result in appearance of local defects ("holes") between the neighbouring molecules [35]. Frequency of appearance of these hollow spaces is determined by the energy of lipid interactions. Since EC6 is characterized by the greatest size (~1.9 nm) among europium chelates under study, it can be assumed that this drug moves apart lipid molecules, thereby creating local "holes". DPH, being entrapped in these defects, experiences more free rotation which manifests itself in the observed decrease of DPH anisotropy in PC_{EC6} liposomes compared to neat PC bilayer.

Table 1 Spectral parameters of DPH, pyrene and Prodan in PC membranes in the presence and absence of europium complexes

	DPH fluorescence anisotropy	Pyrene		Prodan
		I_I/I_{III}	E/M	*3wGP*
Without EC	0.129±0.006	1.115±0.055	0.858±0.043	−0.238±0.012
EC1	0.163±0.008	1.254±0.063	0.418±0.021	−0.151±0.008
EC3	0.156±0.008	1.281±0.064	0.346±0.017	−0.187±0.009
EC6	0.112±0.006	1.385±0.069	0.312±0.016	−0.102±0.005

Pyrene Excimerization Study

Due to its specific spectral properties pyrene represents one of the widely used membrane probes [36–40]. It possesses an ability to form a transient excited-state complex known as "excimer" between the excited and ground-state probe molecules [41]. Pyrene monomers are supposed to be located in glycerol backbone region near lipid headgroups, while excimers are immersed in hydrocarbon membrane core [42]. Relative intensity of monomer emission bands (I_I/I_{III} where I_I and I_{III} are pyrene fluorescence intensities at 374 nm and 384 nm, respectively) is highly sensitive to environmental polarity. Another informative parameter that can be derived from pyrene fluorescence spectra is excimer-to-monomer intensity ratio (E/M) defined as the ratio of fluorescence intensities of monomer (at 392 nm) and excimer (at 470 nm) peaks. E/M reflects the frequency of monomer collisions and, consequently, the rate of excimer formation which depends on membrane free volume.

EC incorporation into PC bilayer was followed by pyrene fluorescence decrease, with the effect being much more pronounced for excimer part of emission spectra (Fig. 2). As seen in Table 1, EC inclusion in the liposomal membranes resulted in the rise of I_I/I_{III}, with the magnitude of this effect becoming greater with increasing EC size. This finding can be rationalized in terms of increased environmental polarity. Bulky EC molecules are likely to move apart neighbouring lipids, thereby favouring water penetration into inner membrane region. On the contrary, EC give rise to E/M decrease in a similar size-dependent manner (Table 1). It can be assumed that EC

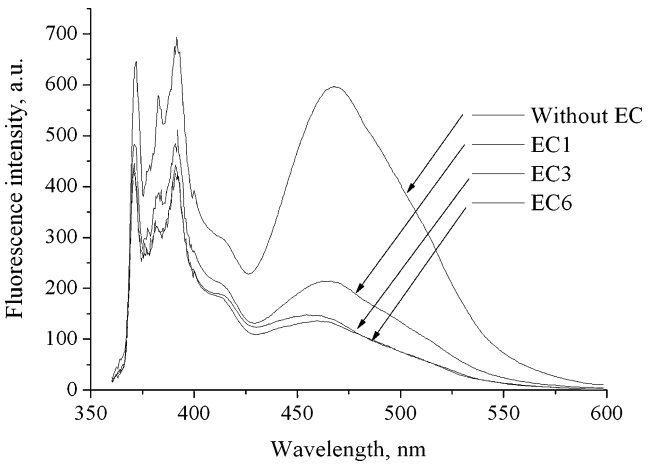

Fig. 2 Pyrene fluorescence spectra in PC model membranes (A), EC-induced increase of first to third vibronic bands ratio in pyrene fluorescence spectra,% (B), EC-induced decrease of excimer-to-monomer fluorescence intensity ratio,% (C). Lipid and pyrene concentrations were 5 μM and 1 μM, respectively. Lipid-to-EC molar ratio was 50:1

induce tighter packing of lipid chains coupled with reduction of the membrane free volume, slowing down pyrene lateral diffusion and decreasing the rate of excimer formation.

Prodan Fluorescence Study

Prodan is a neutral amphiphilic fluorophore which is widely used in the studies of lipid bilayer structural state, polarity, phase transitions and influence of different factors on membrane properties [31, 43–46]. This probe is highly sensitive to the changes in molecular organization and polarity of lipid bilayer. Prodan fluorescence spectrum in water has the maximum at 520 nm, while the probe binding to membranes is followed by the emergence of additional two bands. The short-wavelength band is centered at *ca.* 435 nm and corresponds to Prodan species located at low polar environment at the boundary between hydrophilic and hydrophobic bilayer regions, around glycerol backbone and initial acyl chain carbons. The long-wavelength band has the maximum at *ca.* 480 nm and is attributed to the dye population residing in high polar environment in the vicinity of phosphate groups. Changes in the polarity of probe microenvironment alter the ratio between the above emission bands and, as a consequence, the shape of Prodan fluorescence spectra.

As shown in Fig. 3, EC inclusion into PC model membranes brings about the changes in the contour of Prodan fluorescence spectra. More specifically, pronounced peak at 520 nm which corresponds to Prodan emission in water appears, suggesting that EC promote the probe displacement from lipid to aqueous phase. For more detailed analysis changes in the shape of Prodan emission spectra were quantified by calculating the three-wavelength generalized polarization (*3wGP*), allowing subtraction of free dye contribution to overall spectrum [43]:

$$3wGP = \frac{R_{12}-1}{R_{12}+1}, R_{12} = \frac{I_1 k_{32}}{I_2 k_{32} - I_3 + I_1 R_{31}}, k_{32} = \frac{I_{3W}}{I_{2W}}, R_{31} = \frac{I_{3M}}{I_{1M}} \quad (1)$$

where I_1, I_2, I_3 are Prodan fluorescence intensities at 435, 480 and 520 nm, respectively, subscripts W and M denote aqueous and membrane phases, respectively.

EC addition to liposomes was followed by the decrease of absolute *3wGP* value (Table 1). This effect can be explained by EC ability to reduce polarity of Prodan environment. However, this explanation seems to contradict the above assumption deduced from the analysis of vibronic structure of pyrene fluorescence spectra. This discrepancy can be rationalized in the following way. Prodan-membrane binding is rather weak and can be easily disrupted [46]. It cannot be excluded that EC cause Prodan molecules located closer to the membrane surface to come out from lipid bilayer into water phase. This can lead to the observed decrease in overall polarity of Prodan membrane environment.

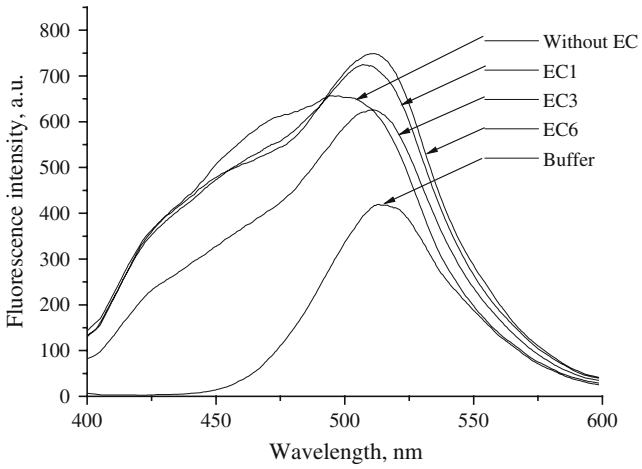

Fig. 3 Emission spectra of Prodan in PC model membranes. Lipid and Prodan concentration were 0.1 mM and 0.86 μM, respectively. Lipid-to-EC molar ratio was 50:1

Binding of Long-Wavelength Dyes to PC Liposomes

Due to high versatility of physicochemical properties and ability to bring together therapeutic, targeting and imaging compounds, liposomes represent an ideal candidate for producing nanocarriers with a number of coordinated specialized functions. In view of this it seemed of interest to ascertain whether EC can be encapsulated into liposomes together with visualizing agents. In this respect particular attention is currently given to NIR fluorophores, which permit overcoming the problems associated with Rayleigh and Raman scattering and attenuating background emission from fluorescent impurities in the analyzed sample.

At the last step of the study we examined the binding of NIR dyes, three squaraines (SQ-1, SQ-2, SQ-3) and one cyanine probe (V2) to EC-free and EC-loaded PC liposomes. Squaraine and cyanine dyes absorb light at 620–685 nm and emit fluorescence at 650–750 nm. They have large Stokes shift, high quantum yield and chemical stability. These attractive spectral properties underlie a wide range of applications of squaraines and cyanines, such as photodynamic therapy [47], biochemical labeling [48], nonlinear optics [49], organic solar cells [50], photoconductors [51], detection of metal ions [52], etc.

Association of NIR dyes with PC liposomes was followed by enhancement of their fluorescence with the magnitude of this effect being increased with lipid concentration. To derive the dye-lipid bilayer partition coefficients in the absence and presence of EC the

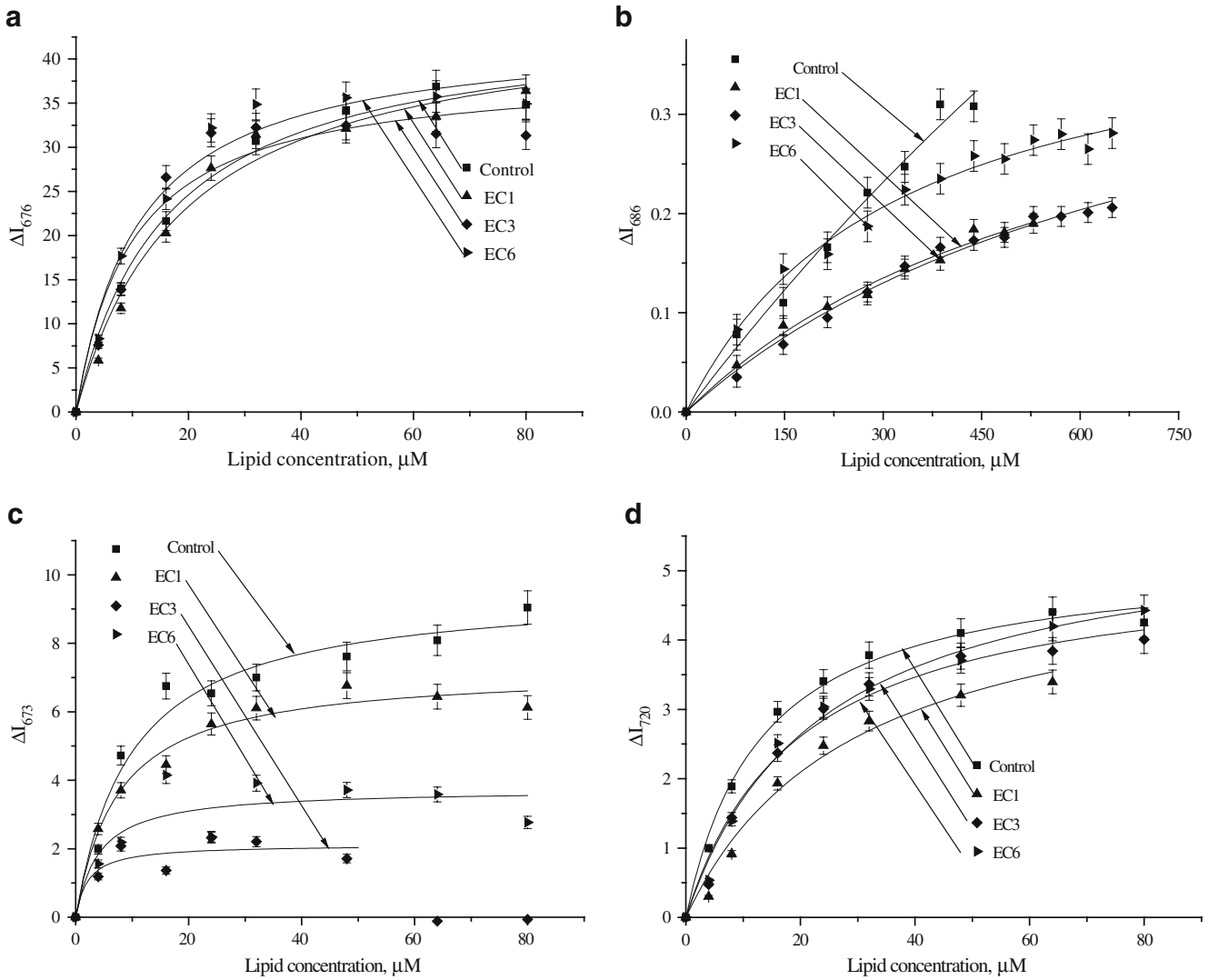

Fig. 4 The isotherms of SQ-1 (**a**), SQ-2 (**b**), SQ-3 (**c**) and V2 (**d**) binding to PC model membranes. Probe concentrations were 0.068 μM (SQ-1), 1.2 μM (SQ-2), 0.02 μM (SQ-3) and 0.27 μM (V2). Lipid-to-EC molar ratio was 50:1. *Solid lines* represent theoretical curves providing the best fit of experimental data. Shown in inset are chemical structures of SQ-1 (**a**), SQ-2 (**b**), SQ-3 (**c**) and V2 (**d**)

experimental dependencies of fluorescence intensity changes on lipid concentration (Fig. 4) were approximated by the following equation:

$$\Delta I = \frac{K_p N_A C_L v_{PC}(I_{\max} - I_W)}{1 + K_p N_A C_L v_{PC}} \quad (2)$$

where K_p is partition coefficient, C_L is molar lipid concentration, v_{PC} is PC molecular volume taken as 1.58 nm^3, N_A is Avogadro's number, I_W is the dye fluorescence in buffer, $I_{\max}$ is a limit fluorescence in a lipidic environment.

As seen from Table 2, partitioning of squaraine dyes into PC membranes is not affected by EC1, but is enhanced in the presence of EC3 and EC6. In the meantime, V2 partition coefficient exhibited lower values in PC_{EC} liposomes compared to neat PC liposomes. It can be supposed

Table 2 Partition coefficients of NIR dyes into PC bilayer

	SQ-1	SQ-2	SQ-3	V2
Without EC	$(6.5\pm1.0)\times10^4$	$(4.7\pm0.9)\times10^2$	$(1.1\pm0.2)\times10^5$	$(7.9\pm0.8)\times10^4$
EC1	$(5.5\pm1.0)\times10^4$	$(1.6\pm0.4)\times10^3$	$(1.4\pm0.2)\times10^5$	$(6.6\pm0.8)\times10^4$
EC3	$(1.0\pm0.3)\times10^5$	$(9.3\pm2.8)\times10^2$	$(2.6\pm0.7)\times10^5$	$(5.4\pm0.9)\times10^4$
EC6	$(9.3\pm1.8)\times10^4$	$(3.0\pm0.5)\times10^3$	$(4.9\pm0.9)\times10^5$	$(4.5\pm0.6)\times10^4$

that EC incorporation into PC bilayer alters packing density of lipid headgroups, allowing greater number of squaraine molecules to penetrate into the membrane polar region. On the contrary, V2, possessing the highest hydrophobicity among the dyes in question, can compete for membrane binding sites in nonpolar membrane core. Likewise, EC-induced increase in packing density of lipid tails may prevent penetration of V2 molecules into hydrophobic bilayer region. Thus, our findings suggest that squaraine dyes can be incorporated into PC membranes in combination with europium chelates. Importantly, squaraines can act not only as visualizing agents, but also as photosensitizing compounds.

In conclusion, the present study has been undertaken to investigate the interaction between the new potential antineoplastic drugs, europium coordination complexes, and model bilayer membranes, composed of zwitterionic lipid phosphatidylcholine. Using fluorescent probes pyrene, 1,6-diphenyl-1,3,5-hexatriene and Prodan, it has been demonstrated that europium chelates incorporated into PC bilayer exert modifying effects on both polar and nonpolar membrane parts. As follows from the analysis of vibronic structure of pyrene fluorescence spectra, EC promote penetration of water molecules into membrane interior. Prodan, another polarity-sensitive probe, reported decrease of bilayer polarity in the presence of europium chelates. This finding was explained by EC ability to squeeze out shallower located probe molecules into aqueous phase. Pyrene excimerization studies revealed EC ability to produce a tighter packing of lipid acyl chains. DPH anisotropy measurements showed that EC size largely determines perturbing effect of these compounds on hydrophobic bilayer region. The finding that the magnitude of bilayer perturbations produced by EC is rather low, together with the observation that EC can be co-encapsulated into liposomes with potential vizualizing agents, squaraine dyes, provide solid background for development of multi-functional liposomal formulations of europium chelates as a novel class of antitumor drugs.

This work was supported by the grant # 4534 from the Science and Technology Center in Ukraine.

References

1. Drulis-Kawa Z, Dorotkiewicz-Jach A (2010) Liposomes as delivery systems for antibiotics. Int J Pharm 387(1–2):187–198
2. Silva-Barcellos NM, Caligiorne S, dos Santos RAS, Frezard F (2004) Site-specific microinjection of liposomes into the brain for local infusion of a short-lived peptide. J Control Release 95 (2):301–307
3. Loa Y, Tsaib J, Kuo J (2004) Liposomes and disaccharides as carriers in spray-dried powder formulations of superoxide dismutase. J Control Release 94(2–3):259–272
4. Gürsoy A, Kut E, Özkırımlı S (2004) Co-encapsulation of isoniazid and rifampicin in liposomes and characterization of liposomes by derivative spectroscopy. Int J Pharm 271(1–2):115–123
5. Trotta M, Peira E, Carlotti ME, Gallarate M (2004) Deformable liposomes for dermal administration of methotrexat. Int J Pharm 270(1–2):119–125
6. Arcon I, Kodre A, Abra RM, Huangd A, Vallner JJ, Lasic DD (2004) EXAFS study of liposome-encapsulated cisplatin. Colloids Surf B 33(3–4):199–204
7. Santos ND, Cox KA, McKenzie CA, van Baarda F, Gallagher RC, Karlsson G, Edwards K, Mayer LD, Allen C, Bally MB (2004) pH gradient loading of anthracyclines into cholesterol-free liposomes: enhancing drug loading rates through use of ethanol. Biochim Biophys Acta 1661(1):47–60
8. Zhang JA, Xuan T, Parmar M, Ma L, Ugwu S, Ali S, Ahmad I (2004) Development and characterization of a novel liposome-based formulation of SN-38. Int J Pharm 270(1–2):93–107
9. Wu P-C, Tsai Y-H, Liao C-C, Chang J-S, Huang Y-B (2004) The characterization and biodistribution of cefoxitin-loaded liposomes. Int J Pharm 271(1–2):31–39
10. Manosroi A, Kongkaneramit L, Manosroi J (2004) Stability and transdermal absorption of topical amphotericin B liposome formulations. Int J Pharm 270(1–2):279–286
11. Zhang JX, Zalipsky S, Mullah N, Pechar M, Allen TM (2004) Pharmaco attributes of dioleoylphosphatidylethanolamine/cholesterylhemisuccinate liposomes containing different types of cleavable lipopolymers. Pharmacol Res 49(2):185–198
12. Ishida T, Ichikawa T, Ichihara M, Sadzuka Y, Kiwada H (2004) Effect of the physicochemical properties of initially injected liposomes on the clearance of subsequently injected PEGylated liposomes in mice. J Control Release 95(3):403–412
13. Scheffold S, Benoit J-P, Leroux J-C, Roux E, Passirani C (2004) Serum-stable and long-circulating, PEGylated, pH-sensitive liposomes. J Control Release 94(2–3):447–451
14. Hemmila I, Laitala V (2005) Progress in lanthanides as luminescent probes. J Fluoresc 15(4):529–541
15. Cummins CM, Koivunen ME, Stephanian A, Gee SJ, Hammock BD, Kennedy IM (2006) Application of europium(III) chelate-dyed nanoparticle labels in a competitive atrazine fluoroimmunoassay on an ITO waveguide. Biosens Bioelectron 21(7):1077–1085
16. Matsumoto K, Nojima T, Sano H, Majima K (2002) Fluorescent lanthanide chelates for biological systems. Macromol Symp 186 (1):117–121
17. Mignet N, le Masne de Chermont Q, Randrianarivelo T, Seguin J, Richard C, Bessodes M, Scherman D (2006) Liposome biodistribution by time resolved fluorimetry of lipophilic europium complexes. Eur Biophys J 35(2):155–161
18. Prosser RS, Bryant H, Bryant RG, Vold RR (1999) Lanthanide chelates as bilayer alignment tools in NMR studies of membrane-associated peptides. J Magn Reson 141(2):256–260
19. Gudasi KB, Havanur VC, Patil SA, Patil BR (2007) Antimicrobial Study of Newly Synthesized Lanthanide(III) Complexes of 2-[2-hydroxy-3-methoxyphenyl]-3-[2-hydroxy-3-methoxybenzylamino]-1,2-dihydroquinazolin-4(3H)-one. Met-Based Drug 2007:37348
20. Fricker SP (2006) The therapeutic application of lanthanides. Chem Soc Rev 35(6):524–533
21. Kostova I, Momekov G, Tzanova T, Karaivanova M (2006) Synthesis, characterization, and cytotoxic activity of new lanthanum (III) complexes of bis-coumarins. Bioinorg Chem Appl 2006:25651
22. Momekov G, Deligeorgiev T, Vasilev A, Peneva K, Konstantinov S, Karaivanova M (2006) Evaluating of the cytotoxic and pro-apoptotic activities of Eu(III) complexes with appended DNA

intercalators in a panel of human malignant cell lines. Med Chem 2(5):439–445
23. Kim SH, Hwang SH, Kim JJ, Yoon CM, Keun SR (1998) Syntheses and properties of functional aminosquarylium dyes. Dyes Pigm 37(2):145–154
24. Ros-Lis JV, Martinez-Manez R, Sancenon F, Soto J, Spieles M, Rurack K (2008) Squaraines as reporter units: insights into their photophysics, protonation, and metal-ion coordination behaviour. Chem Eur J 14(32):10101–10114
25. Mui B, Chow L, Hope MJ (2003) Extrusion technique to generate liposomes of defined size. Meth Enzymol 367:3–14
26. Bartlett G (1959) Phosphorus assay in column chromatography. J Biol Chem 234(3):466–468
27. Lakowicz JR (2006) Principles of fluorescence spectroscopy. Plenum, New York
28. Xiaocui M, Yinlin S, Kechun L, Songqing N (2002) The effect of fibrillar Aβ1-40 on membrane fluidity and permeability. Prot Peptide Letters 9(2):173–178
29. Pebay-Peyroula E, Dufourc EJ, Szabo AG (1994) Location of diphenyl-hexatriene and trimethylammoniumdiphenyl-hexatriene in dipalmitoylphosphatidylcholine bilayers by neutron diffraction. Biophys Chem 53(1–2):45–56
30. Davenport L, Dale RE, Bisby RH, Cundall RB (1985) Transverse location of the fluorescent probe 1, 6-diphenyl-1, 3, 5-hexatriene in model lipid bilayer membrane systems by resonance excitation energy transfer. Biochemistry 24(15):4097–4108
31. Pap EHW, ter Horst JJ, van Hoek A, Visser AJWG (1994) Fluorescence dynamics of diphenyl-1, 3, 5hexatrienelabeled phospholipids in bilayer membranes. Biophys Chem 48(3):337–351
32. Goldstein DB (1984) The effects of drugs on membrane fluidity. Annu Rev Pharmacol Toxicol 24:43–64
33. Arora A, Raghuraman H, Chattopadhyay A (2004) Influence of cholesterol and ergosterol on membrane dynamics: a fluorescence approach. Biochem Biophys Res Commun 318(4):920–926
34. Repáková J, Holopainen JM, Morrow MR, McDonald MC, Čapková P, Vattulainen I (2005) Influence of DPH on the structure and dynamics of a DPPC bilayer. Biophys J 88 (5):398–3410
35. Dobretsov GE (1989) Fluorescent probes in the studies of cells, membranes and lipoproteins. Nauka, Moscow
36. Kalyanasundaram K, Thomas JK (1977) Environmental effects on vibronic band intensities in pyrene monomer fluorescence and their application in studies of micellar systems. J Am Chem Soc 99(7):2039–2044
37. Sugar IP, Zeng J, Chong PL-G (1991) Use of Fourier transforms in the analysis of fluorescence data. 3. Fluorescence of pyrene-labeled phosphatidylcholine in lipid bilayer membrane. A three-state model. J Phys Chem 95(19):7524–7534
38. Fischkoff S, Vanderkooi JM (1975) Oxygen diffusion in biological and artificial membranes determined by the fluorochrome pyrene. J Gen Physiol 65(5):663–676
39. Valeur B (2002) Molecular fluorescence: principles and applications. Wiley-VCH, Weinheim
40. Tedeschi C, Möhwald H, Kirstein S (2001) Polarity of layer-by-layer deposited polyelectrolyte films as determined by pyrene fluorescence. J Am Chem Soc 123(5):954–960
41. Duportail G, Lianos P (1996) In: Rosof (ed) Vesicles. Marcel Dekker, New York, pp 295–371
42. Barenholz Y, Cohen T, Haas E, Ottolenghi M (1996) Lateral organization of pyrene-labeled lipids in bilayers as determined from the deviation from equilibrium between pyrene monomers and excimers. J Biol Chem 271(6):3085–3090
43. Krasnowska EK, Gratton E, Parasassi T (1998) Prodan as a membrane surface fluorescence probe: partitioning between water and phospholipid phases. Biophys J 74(4):1984–1993
44. Wilson-Ashworth HA, Bahm Q, Erickson J, Shinkle A, Vu MP, Woodbury D, Bell JD (2006) Differential detection of phospholipid fluidity, order, and spacing by fluorescence spectroscopy of bis-pyrene, Prodan, nystatin, and merocyanine 540. Biophys J 91(11):4091–4101
45. Parasassi T, Giusti AM, Gratton E, Monaco E, Raimondi M, Ravagnan G, Sapora O (1994) Evidence for an increase in water concentration in bilayers after oxidative damage of phospholipids induced by ionizing radiation. Int J Radiat Biol 65(3):329–334
46. Parasassi T, Krasnowska EK, Bagatolli L, Gratton E (1998) Laurdan and Prodan as polarity-sensitive fluorescent membrane probes. J Fluoresc 8(4):365–373
47. Jyothish K, Avirah RR, Ramaiah D (2007) Development of squaraine dyes for photodynamic therapeutical applications: synthesis and study of electronic factors in the dye formation reaction. ARKIVOC 8(viii):296–310
48. Renard B-L, Aubert Y, Asseline U (2009) Fluorinated squaraine as near-IR label with improved properties for the labeling of oligonucleotides. Tetrahedron Lett 50(17):1897–1901
49. Yang GC, Shi SQ, Guan W, Fang L, Su ZM (2006) Hyperpolarizabilities of para-nitroaniline and bis[4-(dimethylamino) phenyl] squaraine: the effects of functional/basis set based on TDDFT–SOS method. J Mol Struct 273(1–3):9–14
50. Inoue T, Pandey SS, Fujikawa N, Yamaguchi Y, Hayase S (2010) Synthesis and characterization of squaric acid based NIR dyes for their application towards dye-sensitized solar cells. J Photochem Photobiol A 213(1):23–29
51. Pacanskya J, Waltmana RJ, Coufala H, Cox R (1988) New methods for preparing organic layered photoconductors. Int J Radiat Appl Instrum C 31(4–6):853–875
52. Chandrasekaran Y, Dutta GK, Kanth RB, Patil S (2009) Tetrahydroquinoxaline based squaraines: synthesis and photophysical properties. Dyes Pigm 83(2):162–167